ELSEVIER

Chemical Geology 194 (2003) 119–141

CHEMICAL GEOLOGY
INCLUDING
ISOTOPE GEOSCIENCE

www.elsevier.com/locate/chemgeo

Mixing of metamorphic and surficial fluids during the uplift of the Hercynian upper crust: consequences for gold deposition

Marie-Christine Boiron[a,*], Michel Cathelineau[a], David A. Banks[b], Serge Fourcade[c], Jean Vallance[a]

[a] *CREGU and UMR G2R CNRS 7566, BP 23, 54501 Vandoeuvre lès Nancy cedex, France*
[b] *School of Earth Sciences, University of Leeds, Woodhouse Lane, Leeds LS2 9JT, UK*
[c] *UMR CNRS 6118 Géosciences Rennes, Campus de Beaulieu, Av. du G[al] Leclerc, 35042 Rennes cedex, France*

Abstract

A detailed geochemical study of fluids from representative quartz-sealed faults hosting late Hercynian gold concentrations shows that fluids percolating the mineralised faults had two main distinct reservoirs: one was a quite shallow and the other rather deep-seated. Both fluids have lost a great part of their original geochemical signature through interactions with host metamorphic formations. Early fluids, present during the primary sealing of the faults by quartz, are considered to have effectively equilibrated with the metamorphic pile and then predominantly flowed upwards along the faults. They are characterised by $CH_4/CO_2/H_2O$ ratios rather typical of fluids equilibrated with graphite, and moderate to medium chlorinities with a high Br/Cl ratio. The striking feature of the gold-bearing quartz is that gold is not synchronous within any quartz deposition, and appears located in late microfractures and associated with Pb–Bi–Sb sulphosalts and sulphides. These late stages are characterised by fluids whose salinities decrease to very low values indicating their progressive dilution by waters of more surficial origin in the fault system.

The long-lived activity of the fault favoured the connection between two distinct fluid reservoirs at a critical time during the basement uplift. The fluids evolved through two main driving mechanisms which were responsible for the Au deposition: (i) decrease in temperature accompanying decompression from supra-lithostatic to hydrostatic conditions which yielded, in some instances, volatile unmixing in the faulted systems, (ii) mixing of the resulting fluids with waters entering the hydrological systems from shallower reservoirs. In addition to dilution and fluid mixing which are favourable factors for decreasing the gold solubility, the presence of microfractured sulphides could have enhanced gold precipitation through electrochemical processes.

Keywords: Gold; Fluid chemistry; Stable isotopes; *P–T* conditions; Uplift; Variscan belt

1. Introduction

Previous case studies of Au–(As) ore deposits in the Variscan belt of western Europe have shown that they formed under similar conditions during the late stages of uplift (Boiron et al., 1990; Noronha et al., 2000). Most mineralised structures are faults sealed by

* Corresponding author. Tel.: +33-3-83-68-47-30; fax: +33-3-83-68-47-01.
E-mail address: marie-christine.boiron@g2r.uhp-nancy.fr (M.-C. Boiron).

0009-2541/02/$ - see front matter © 2002 Elsevier Science B.V. All rights reserved.
PII: S0009-2541(02)00274-7

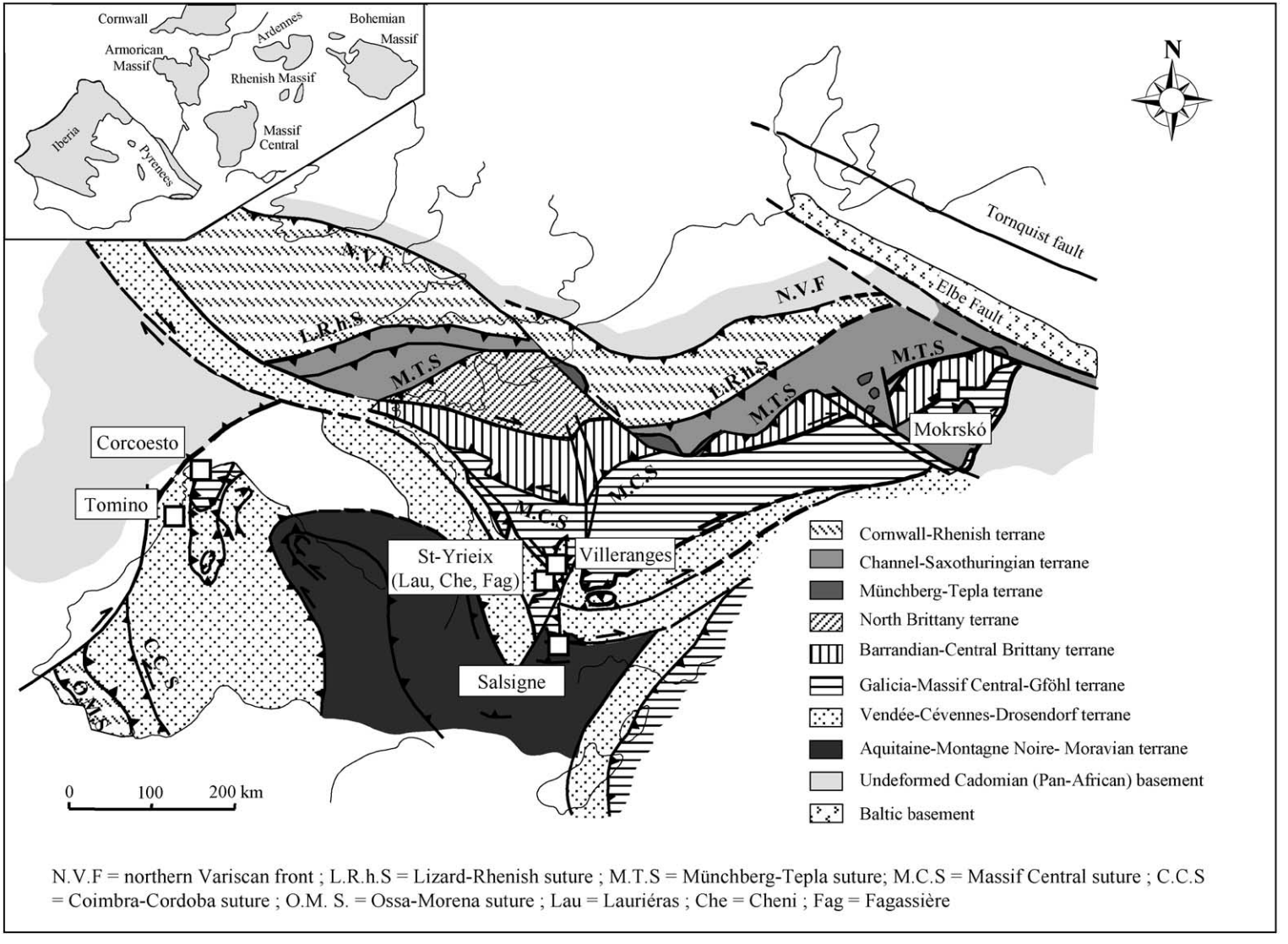

Fig. 1. General map of the Variscan range in Western Europe with location of the studied ore deposits (modified from Matte, 1991).

quartz that was deposited from volatile-rich fluids, but experienced a complex evolution combining ductile then brittle deformation during uplift (Boiron et al., 1996). In contrast with most Archean Au-lodes (Groves, 1993), mineralised quartz faults are characterised all over Europe by a long-lived structural evolution revealed by macro- and microstructures inherited from various superimposed brecciation, fracturing, sealing or healing stages (Bouchot et al., 2000). Thus, crack-seal textures commonly described in Archean lode deposits (Robert and Brown, 1986; Dugdale and Hagemann, 2001) are generally lacking in late Hercynian deposits. Gold-hosting material in the latter deposits rather consists of breccia made of milky quartz cemented by fine-grained quartz which, in turn, is affected by microfracturing. Microfractures are frequently healed as fluid inclusion planes but sometimes are filled with hyaline quartz (Boiron et al., 1992). The succession of mineral assemblages and fluid types defines a unique cycle of fluid evolution in most studied faults. The apparent similarity of the processes at the scale of the whole European province of Hercynian gold deposits provides the opportunity to synthesise fluid geochemistries and sources in an attempt to build up a generalised model of fluid production and flow regimes during the late uplift stage of a collisional orogen.

This present paper compares the characteristics of fluids involved in some important crustal structures mineralised in Au and As throughout western Europe (Fig. 1) namely: (i) in ''mesothermal'' gold deposit fluids (quartz veins in the gold-bearing Saint-Yrieix district (Bouchot et al., 1989; Boiron et al., 1990, 1992; Essarraj et al., 2001), in the Salsigne district (Cathelineau et al., 1993), in North Iberia (Galicia) (Boiron et al., 1996; Arias and Martin-Izard, 2000) and in the Bohemian Massif (Moravek et al., 1989; Boiron et al., 2001) and (ii) fluids associated with shallow ''epithermal'' mineralisation (As, Au) in volcano–sedimentary series (Marche-Combrailles; Boiron et al., 1989; Cathelineau et al., 1989). Paragenetic mineral associations before and during the ore deposit stage, related chemical evolution as well as gold distribution were simultaneously considered in order to unravel the physical/chemical factors controlling the gold ore-forming processes.

The present synthesis uses a multitechnique database from fluid inclusions that was systematically built up on the aforementioned Au–As ore deposits combined with microstructural and ore mineral paragenesis. New data are reported on individual inclusions (microthermometry, Raman spectroscopy) together with new analyses of bulk leachates and oxygen isotope geochemistry on quartz from the same (bulk and sometimes microscopic) samples.

2. Geological setting

2.1. The French Massif Central

2.1.1. The Saint-Yrieix district

This district is a major metalliferous province of the Variscan belt with several deposits such as Lauriéras, Bourneix, Moulin de Cheni, La Fagassière which formed during the intense hydrothermal activity that characterised the Neo-Variscan period (320–290 Ma) (Marignac and Cuney, 1999). The gold deposits are located in the Northwestern part of the French Massif Central, 40 km south of Limoges. This area displays series of 0.1- to 1-km long fault zones oriented NE–SW, locally hosting quartz lenses, the length of which are typically in the 10 to 100 m range (Bouchot et al., 1989; Touray et al., 1989). This district, still mined today, has already produced around 45 tons of gold metal.

The lower lithotectonic unit of the Limousin gneisses hosting the deposits is composed of micaschists of probable Late Precambrian age and of Early Paleozoic (490 Ma) orthogneisses. The basement of central Limousin consists of a pile of metamorphic thrust sheets emplaced during the Early Devonian (Floc'h, 1983). Three main stages of metamorphism and deformation are distinguished: (i) an early high temperature (620 °C)–high pressure (500 MPa) stage, followed by (ii) a major Barrovian stage and finally, (iii) a Carboniferous event (Floc'h, 1983) characterised by the intrusions of peraluminous granites (ca. 320–330 Ma; Duthou et al., 1984).

The major faults hosting the gold-bearing quartz structures strike 70±20°N, with a 60±10°NW dip, and crosscut a series of gneisses with amphibolite or leptynite intercalations, characterised by a flat-lying foliation (5–20° dip). Peraluminous fine-grained granites intrude the gneisses as small sills or veins and do not display any significant magmatic or ductile deformation features.

This main studied site was the Lauriéras system of quartz lenses which has yielded relatively high-grade ores around 25 g Au/ton. The main fault infillings in "Laurieras" display the textures typical of Au-mineralised quartz veins in the French Massif Central, comparable with the "Bourneix" Au-bearing quartz system (Hubert, 1986; Bouchot et al., 1989). New data on two other gold-bearing structures, "Moulin de Cheni" and "La Fagassiere", are also discussed.

2.1.2. The Salsigne district

The Salsigne district, located in the southern part of the French Massif Central, is an important gold province with the Salsigne mine still active and numerous gold showings (120 tons of gold metal extracted since 1924). The main Salsigne deposit is hosted by metamorphic series including Cambrian and Devonian limestones and Early Cambrian detrital rocks (arkosic sandstones) (Tollon, 1969; Lepine, 1989). Early sulphides (pyrrhotite and arsenopyrite) occur in microfractured rocks close to shear planes, together with milky quartz and are affected by ductile–brittle deformation considered as late Westphalian–Middle Stephanian (Lescuyer et al., 1993).

2.1.3. The Marche-Combrailles area

Along the Marche-Combrailles shear zone (Northwestern part of the French Massif Central; Boiron et al., 1989), Au showings and deposits lie within a 50-km long zone. Gold ores occurs in the Hercynian basement (Guéret monzogranite and anatectic biotite–cordierite gneisses), the Visean volcano–sedimentary basins and late intrusions of peraluminous granites and calc-alkaline lamprophyres. The deposits consist of shallow "epithermal mineralisation" (Au-bearing arsenopyrite and, to a minor extent, pyrite) found within both the volcano–sedimentary series (Villeranges; Boiron et al., 1989) and the Hercynian basement (Chatelet; Zappettini, 1983, Piantone et al., 1994). These formed during a late stage of brittle deformation that was significantly later than the formation of the continental basin.

2.2. The Bohemian Massif

The Psí Hory gold district (Mokrsko and Celina deposits) is located in Central Bohemia, approximately 50 km south of Prague, in the contact zone between Hercynian intrusives (the Mokrsko granodiorite) and Upper Proterozoic metamorphic rocks from the Jílové belt. The Jílové belt is a linear structure (70 km long and up to 6 km wide) of Upper Proterozoic age (640–700 Ma) which consists of a bimodal volcano–sedimentary complex exhibiting both tholeïtic and calc-alkaline trends. These geological units have undergone regional metamorphism to greenschist facies during the Cadomian orogeny (550–650 Ma). During the early phase of the Variscan orogeny (320–360 Ma), differentiated granitic rocks, mostly granodiorites, quartz diorites and tonalites, markedly contaminated in places by the assimilation of volcanic and sedimentary rocks of Upper Proterozoic age intrude the metamorphic series.

The Mokrsko ore zone (Moravek et al., 1989) is an east–west trending zone, several hundred meters thick, characterised by abundant dilational fractures. Thus, in the ore zone, a dense set of subparallel quartz–arsenopyrite veinlets penetrates the granodiorite (Boiron et al., 2001). The main ore zones occur where the quartz veinlets are the densest. The quartz veinlets and the granodiorite have subsequently been affected by a succession of brittle deformation events responsible for the development of microfissure sets (mostly fluid inclusion planes).

2.3. The NW Iberian zone

The NW part of the Iberian Peninsula is characterised by extensive areas of Hercynian basement, mostly composed of Paleozoic metasedimentary rocks and Variscan granites. Several areas display extensive sets of quartz veins formed during late brittle deformation stages within the granite. The best examples are associated with the major Malpica–Vigo shear zone, which is located in the western part of Galicia, Spain (Arias and Martin-Izard, 2000). Two representative areas have been investigated. The Corcoesto and Tomino (Galicia) deposits are both located along the Malpica–Vigo shear zone that is mostly dextral, except along a small NW–SE segment. The trend of this zone varies from N30°E in the North (Malpica) to N170°E in the South (Vigo) (Iglesias and Choukroune, 1980). In these mining districts, Au–As ores display similar features with specific deformation stages affecting the quartz

veins. Rocks surrounding the granites are mostly pelitic metasediments, often containing graphite. In some instances, graphite is a major rock component (mostly in the Tomino area).

3. Methods

3.1. Fluid petrography

Studies of the typology and petrography of fluid inclusions have been carried out on wafers from representative samples of the host rocks and of the quartz veins. The succession of fluid circulation has been studied by looking at relationships between fluid inclusions, their host mineral and the location of ore minerals in order to obtain information on the relative formation chronology of mineral assemblages as a function of deformation and fluid events. In most deposits, SEM images (back scattered and cathodoluminescence) were obtained to determine the relationships between microfractures in quartz (fluid inclusion planes) and microfractures in sulphides.

The notation of fluid inclusion types follows the nomenclature previously published (Boiron et al., 1992, 1996), which takes into account the nature of the dominant chemical phases (see Table 1). It is based on the quantity of C–H–O–(N–S) species detectable by Raman spectroscopy (subscript c, when CO_2 is dominant; m, when CH_4 is present in significant amounts up to 30–40 mol%); and w for water. The subscripts consist in a combination of the letters related to the abundance of the various species in the fluid.

3.2. Microthermometry and Raman data

Fluid inclusions have been extensively studied and related to the sequence of mineral precipitation within the veins to constrain the conditions of fluid migration and Au deposition.

Microthermometric characterisation of the fluid inclusions was performed on wafers (<300 μm in thickness) using a Chaixmeca heating–freezing stage (Poty et al., 1976). The stage was calibrated with melting-point solid standards at $T>25$ °C and with natural and synthetic inclusions at $T<0$ °C. The rate of heating was monitored in order to obtain an accuracy of ±0.2 °C during freezing, ±1 °C when heating over the 25–400 °C range and ±4 °C over the 400–600 °C range. Salinity, expressed as equivalent wt.% of NaCl, was calculated from microthermometric data using the revised equation of Bodnar (1993).

In volatile-bearing fluid inclusions, CO_2 was identified by melting of a solid below −56.6 °C. The volumetric fraction of the aqueous liquid and the volumetric fraction of the volatile-rich liquid in the volatile-rich phase have been estimated by reference to the volumetric chart of Roedder (1972), in order to reconstruct bulk fluid compositions.

Molar fractions of CO_2, CH_4, H_2S and N_2 were determined in individual inclusions by micro-Raman analysis performed with a Labram Raman spectrometer at CREGU (Nancy). Bulk composition and molar volume were computed from the $P–V–T–X$ proper-

Table 1
Typology and nomenclature of fluid inclusions

Type of fluid inclusions	Dominant species	Remarks
c–w	CO_2–(CH_4–N_2)–H_2O–NaCl	Tm CO_2 and Th CO_2 observed, high density volatile phase, $CH_4+N_2<40$ mol% in the volatile phase
c–m–w	CO_2–CH_4–N_2–H_2O–NaCl	Tm CO_2 and Th CO_2 observed, high density volatile phase, $40<CH_4+N_2<75$ mol% in the volatile phase
w–c	H_2O–CO_2–(CH_4–N_2)–NaCl	Only Tm cl observed, low density volatile phase, $CH_4+N_2<40$ mol% in the volatile phase
w–c–m	H_2O–CO_2–CH_4–N_2–NaCl	Only Tm cl observed, low density volatile phase, $40<CH_4+N_2<80$ mol% in the volatile phase
w	H_2O–NaCl	

Tm CO_2: melting temperature of solid CO_2, Th CO_2: homogenisation temperature of CO_2, Tm cl: melting temperature of clathrate.

ties of individual inclusions in the C–O–H–S system (Dubessy, 1984; Dubessy et al., 1989; Thiery et al., 1994; Bakker, 1997). The $P–V–T–X$ properties of aqueous carbonic inclusions were modelled for the system $H_2O–CO_2–CH_4$ using the equations of state of Kerrick and Jacobs (1981) and Jacobs and Kerrick (1981). For aqueous inclusions, the isochores have been drawn in the H_2O–NaCl system using the data from Zhang and Frantz (1987).

3.3. Fluid electrolyte composition

Bulk crush leach analysis of the inclusion fluid contained within different quartz samples has been carried out in order to characterise their ionic composition and, in particular, to explore the use of halogens as conservative tracers of fluid sources. Although it is clear that individual samples may contain a mixture of different fluid generations, each investigated sample was carefully selected in the light of the microthermometric results to ensure that it was dominated by a single fluid generation.

The crush leach procedure which has been used is that of Bottrell et al. (1988), with modifications described in Yardley et al. (1993). The weight of sample crushed was typically 0.5–1 g. Analysis of Cl, Br and I was performed by ion chromatography on double-distilled water leachates. Raw analyses of the whole leach solutions were recalculated with reference to the mean salinity from microthermometry. The errors in the Br/Cl ratio are less than 10%, while errors associated with the I/Cl ratios are much larger, usually a factor of 2 or 3, due to the low concentrations of I in the leach solutions.

3.4. Isotope geochemistry

Quartz $^{18}O/^{16}O$ ratios were measured using the conventional fluorination method of Clayton and Mayeda (1963). Two types of samples were analysed: (i) bulk quartz samples (ca. 7 mg) and (ii) chips of quartz (down to ca. 1 mg) extracted from the fluid inclusion wafers. These chips correspond exactly to the material on which FI studies were performed. The uncertainties (estimated from duplicates performed on different Ni fluorination tubes) are generally on the order of 0.1‰but may reach 0.25‰ for the quartz chips extracted from fluid inclusion wafers. The reason for that poorer reproducibility may result from the small size of the analysed samples, but also from the fact that quartz crystallised or recrystallised from a hydrothermal fluid may be isotopically heterogeneous on a small scale (two adjacent chips are not necessarily representatives of exactly the same quartz generation or of the same mixture of different quartz types).

4. Quartz veins and gold ores

In all the so-called "mesothermal" late Hercynian deposits, with the exception of the "epithermal" mineralisation of the Marche-Combrailles area, the quartz typology and associated ores follow the same succession. A summary is given in Table 2.

The early quartz matrix is affected by ductile deformation followed by a series of brittle deformational stages identified at the microscopic scale by a succession of quartz types and textures (Boiron et al., 1992, 1996; Essarraj et al., 2001; Vallance, 2001). Several silicification stages occurred in relation with the ductile–brittle to brittle deformation events:

(i) major silicification in the ductile–brittle regime corresponding to the deposition of milky quartz (mkQ) enriched in abundant small (<5 μm) fluid inclusions (quartz lens formation stage);
(ii) brecciation of the milky quartz lens and cementation of the resulting grains by microcrystalline quartz (mQ) in the Saint Yrieix district or crystallisation of clear quartz (cQ) present as bands and overgrowths on mkQ, sometimes with euhedral terminations (Iberian deposits);
(iii) crystallisation of hyaline quartz, sometimes euhedral (hQ), cementing arsenopyrite crystals, cQ and hQ quartz contain scattered primary fluid inclusions and pseudo-secondary fluid inclusions;
(iv) formation of small size fractures during later brittle deformational stages.

During these late stages of fluid migration, fluid inclusion planes result from annealing of microcracks and are observed in all former quartz types. In some instances, low temperature barren quartz (lbQ), as comb and radially disposed crystals, is observed as

Table 2
Summary of the mineralogical assemblages, fluid types and element deposition observed in the studied deposits

French Massif Central				Northwest Iberia		Bohemia	Quartz deposition	Main element deposited	Fluid type	
Lauriéras	Cheni-Fagassière	Salsigne	Villeranges–Chatelet	Corcoesto	Tomino	Mokrsko				
18 t—*30 t*		**120 t**—*30 t*	**10 t**—*20 t*	*30 t*	*10 t*	*100 t*				
pyr–arsp	pyr–arsp	pyr–arsp		pyr–arsp	pyr–arsp–po	pyr–arsp–po	Si-major sealing	As–Fe–S	CO_2–H_2O–(CH_4–N_2)–NaCl CO_2–CH_4–(N_2)–H_2O–NaCl	c–w c–m–w
pyr–arsp (Au) boul (Au) chlorite–phengite	pyr–arsp fk–phengite chlorite	pyr–arsp chlorite		arsp chlorite–phengite	arsp chlorite–phengite	po–cpy–gal chlorite–phengite	(Si)-thin microfractures	As–Fe–S	H_2O–CO_2–(CH_4–N_2)–NaCl	w–c
sph–cpy native Au boul II–gal	sph–cpy native Au boul II–gal	cpy native Au–gal Bi–bism–chlorite	po–chlorite combined Au in pyr–arsp ankerite–illite stibnite	sph–cpy–gal native Au Cu–Ag sulfosalt Bi–bism	sph–cpy native Au Cu–Zn–As sulfosalt Bi–bism	sph–Te–minerals native Au stibnite Bi–bism chlorite	healing quarts only at Villeranges and Chatelet	Zn–Cu–S Au Pb–Bi–Te–(Sb)	H_2O–NaCl	w
	calcite		calcite			calcite	barren quartz		H_2O–NaCl	w

Approximate extracted Au tonnage (in bold) and estimated reserves (in italic) are given.
pyr: Pyrite, arsp: arsenopyrite, arsp (Au): combined gold in arsenopyrite, boul (Au): combined gold in boulangerite, sph: sphalerite, cpy: chalcopyrite, gal: galena, po: pyrrhotite, bism: bismuthinite, Bi: native Bi, fk: K-feldspar, Si: quartz.

late infillings which postdate As–Au ores. They are related to late openings of the faults (La Fagassière deposit, for instance).

Specific mineral assemblages are associated with a given quartz type and with the late microfissures: (1) phengite, pyrite, massive arsenopyrite (±pyrrhotite in some instances) are included in mQ quartz, (2) euhedral arsenopyrite crystallised on cQ bands prior to hQ quartz growth, (3) chlorite, locally with sulphosalts (Pb–Ag dominated), chalcopyrite, bismuth/bismuthinite, or native gold occur in late microfissures crosscutting all the formerly grown quartz and sulphides. Gold is found dominantly as small metallic particles, mostly in vugs or crack sets, especially where they crosscut earlier sulphides. Deposition of native gold in most of these deposits is most probably the result of electrochemical processes at the surface of crushed sulphides as suggested by Knipe et al. (1991), Möller and Kersten (1994). At Salsigne, gold is typically associated with bismuthinite, sulfosalts and chalcopyrite, and is interpreted to be the result of sulfidation processes (alteration of bismuth and pyrrhotite) together with destabilisation of Fe-silicates (Benchekroun et al., 1996). There is very little evidence of gold input in the earliest stages of veins formation (Q1 to Q3), apart from the presence of gold in a combined state in some growth bands of arsenopyrite and boulangerite (Lauriéras; Essarraj et al., 2001).

In the "epithermal" mineralisation of the Villeranges volcano–sedimentary basin, gold is carried in a combined state within arsenopyrite and pyrite crystals, occurring either within a diffused network of quartz + ankerite veinlets or as isolated crystals in the altered tuffs (illite–quartz–ankerite assemblage). Stibnite occurs either as massive veins or as small needle-shaped crystals associated with ankerite and quartz combs.

5. Fluid characterisation

Two major types of fluids have been recognised in most studied deposits all along the Variscan belt, except Villeranges–Chatelet: (i) dominant CO_2–H_2O-rich fluids, locally enriched in CH_4 near graphite-rich wall rocks, which are generally followed by H_2O–(CH_4–CO_2) liquids having a low-density volatile phase that was trapped after a significant pressure drop, (ii) aqueous fluids (with moderate to low salinities, up to 9 eq. wt.% NaCl) characterised the latest stages of fracturing and fluid infiltration. The latter progressively become predominant in the system. Aqueous fluids are associated with the main ore assemblage Au–Bi/bismuthinite (±Pb, Sb, Cu sulphides or sulphosalts) which occur in cracks within early barren sulphides (mostly arsenopyrite and to a lesser degree, pyrite). These aqueous fluids are generally identified in secondary fluid inclusion planes, especially in the mineralised areas. At Villeranges–Chatelet, aqueous fluids are the only type represented, and are observed as primary inclusions in gangue minerals hosting Au-bearing sulphides.

A summary of the microthermometric and Raman data including bulk compositions is given in Tables 3 and 4.

5.1. Composition of the volatile phase, density and bulk chemical evolution of major components

The early C–H–O–N fluids (c–(±m)–w) have compositions typical of metamorphic environments where graphite is present. They are mostly dominated by CO_2 but locally, these fluids may be extremely enriched in CH_4 and N_2 (up to 30–50 mol%), especially in the proximity of lydites or black shales, indicating that the devolatilisation of C-rich units may be largely responsible for the increase of CH_4. This is particularly the case at the Tomino deposit and, to a lesser degree, at Corcoesto and Lauriéras (Table 4).

Compositional changes in the volatile phase are related to a decrease in its density (dv) (Fig. 2), ranging from values around 0.8 g/cm^3 (three-phase inclusions dominated by CO_2) to 0.2 g/cm^3 (for w–c inclusions). The fluid inclusions with the lowest densities are characterised by the highest water contents (between 90 and 96 mol% H_2O in most of the deposits, except at Mokrsko), a decrease of the CO_2 content and an enrichment in CH_4±N_2. All these features define a characteristic and continuous time evolution. Three main processes involved in this evolution can be distinguished: (i) mixing of the predominantly c–w fluids with CH_4±N_2 fluids of variable CO_2–H_2O content, associated with graphitic-rich lithologies (Fig. 3); (ii) unmixing of the volatiles and the subsequent heterogeneous trapping of the unmixed end-members, already discussed in

Table 3
Summary of the microthermometric characteristics (range and mode) for the aqueous carbonic and aqueous fluids

Location	Fluid type	Tm CO_2	Th CO_2	Mode	Tm cl	Tm ice	Th	Mode
French Massif Central								
Lauriéras (1)	c–w	−62.5/−56.7	6/28	L or V	5.4/12	−5.2/−2	230/390	L or V
		−58/−60			10	−4		
	w–c	−62.3/−57.6	nv		7.5/11.6	−5/−2.3	290/360	L
		−59			11			
	w–c–m	nv	nv		8/14	−4.2/−3.5	320/370	L or V
					13	−4		
Cheni (2)	c–w	−60.9/−56.8	8.6/31	L or V	2.8/10.8	−5.5/−0.6	150/250	L
		−58	25					
	w					−5.2/−0.5	190/210	L
Fagassière (2)	c–w	−58.4/−58.1	28/31	L or C	6.8/7.2	no	305/366	L
		−58.2	29		7			
	w–c	−58.2/−59.5	nv		7.2/9.4	no	280/305	L
		−58.3			9		295	
	w–c–m	−57.4/−67.3	nv		8.3/9.1	no	365	V
		−59.5						
	w					−5.6/−0.8	155/280	L
Salsigne (3)	c–w	−57.4/−59	−12.1/12.6	L	1.5/7.5	−7.2/−4	220/390	L
		−58						
	c–m–w	−60.5/−62.3	−3.6/−6.3	L	no	−6		
		−61.5						
	w					−6.8/−0.5	120/320	L
Villeranges (4)	w (qz–arsp)					−2/−0.3	140/210	L
	w (qz–sb)					−4/−1.2	150/200	L
Chatelet	w (qz–arsp)					−3.3/−0.3	140/240	L
Bohemian Massif								
Mokrsko (5)	c–w	−58.1/−56.6	16/29.8	L or V	5/10	−4.7/−1.1	300/420	L or V
		−57.4	29		7		350	
	w					−6/−0.5	130/280	
						−4.5/−1	160	
Northwest Iberia								
Corcoesto (6)	c–w	−60.6/−56.8	19/30.5	L or V	4/11	−5.6/−2.5	320/390	L or V
		−57.6	24/30		8	−5	350	
	w–c	−60.2/−56.8	nv		6.5/12	−6.8/−2.3	345/390	L or V
		−57.6				−3.5	350	
	w–c–m	−60.3/−58.5	nv		8/10.4	−7.2/−2.4	345/380	L or V
		−59			9	−6	350	
	w					−7/−1	150/300	L
						−4	220	
Tomino (6)	c–w	−60.5/−56.6	4/30	L or V	4/12	−8.7/−6	240/420	L
		−57.5	26		7	−6	350	
	c–m–w	−65.5/−60.5	−16/14	L or V	8/14	−6.1/−2	300/>500	
		−62	−8/+4		11	−5.5		
	w					−4.5/−0.1	145/270	

Data have been completed or synthetised from: 1—Essarraj et al. (2001), 2—Vallance (2001), 3—Boiron et al. (1990), 4—Boiron et al. (1989), 5—Boiron et al. (2001), 6—Boiron et al. (1996).
Tm CO_2: melting temperature of solid CO_2, Th CO_2: homogenisation temperature of CO_2, Tm ice: melting temperature of ice, Tm cl: melting temperature of clathrate, Th: homogenisation temperature. Homogenisation modes: L—liquid and V—vapour. All values are in °C. Nomenclature for fluid inclusions is explained in the text; no: not observed.
Qz–arsp: quartz–arsenopyrite, Qz–sb: quartz–stibnite.

Table 4
Summary of the Raman data and bulk composition for the aqueous carbonic fluids

Location	Fluid type	Raman data			Bulk composition				
		CO_2	CH_4	N_2	H_2O	CO_2	CH_4	N_2	NaCl
French Massif Central									
Lauriéras (1)	c–w	54–96	2–35	nd–25	80–92	5–15	0.1–6	nd–2	0.1–2
	w–c	58–93	7–40	nd–4	90–94	5–8	0.3–3	nd–0.25	0.8–2.5
	w–c–m	34–18	45–66	nd–8	90–94	3–5	1–4.5	nd–0.25	1.5–3
Cheni (2)	c–w	74–10	nd–18	nd–11	69–94	4–28	nd–2.3	nd–1.8	0.2–3.8
Fagassière (2)	c–w	95–98	0.7–1	1.5–4	88–91	7–10	0.05	0.1–0.2	1.2–1.4
	w–c	82–85	3–5.5	10–14	91–93	6–7.5	0.1–0.2	0.4–0.7	0.8–1.1
	w–c–m	19–21	28–30	50–52	77–78	4.5–5.5	6–6.5	10.5–11.5	*
Salsigne (3)	c–w	60–96	4–33	nd–6	22–98	2–77	0.1–25	nd–4	0.5–2.5
	c–m–w	20–55	40–76	3–15	25–94	4–42	1–50	0.1–11	1.5–3
Bohemian Massif									
Mokrsko (4)	c–w	89–99	nd–6.8	nd–10.8	16–84	13–83	nd–2.7	nd–3.2	0.2–2.1
Northwest Iberia									
Corcoesto (5)	c–w	72–100	1–23	nd–10.5	40–85	13–58	nd–2.5	nd–1.3	0.5–2.6
	w–c	65–95	4–32	nd–7	93–95	4–5	0.7–2	nd–0.2	0.2–1
	w–c–m	50–52	44–45	2–3	95–96	1.8–2	1.6–1.8	0.1	0.4–0.6
Tomino (5)	c–w	76–100	nd–22	nd–10	40–92	5–59	nd–6	nd–2.7	0.2–2
	w–c–m	40–70	23–60	nd–10	30–92	3–37	1–26	nd–4	0.4–2.7

For each fluid inclusion type, ranges of compositions are given in mole %. Nomenclature for fluid inclusions is explained in the text; nd: not detected.
Data have been completed or synthetised from: 1—Essarraj et al. (2001), 2—Vallance (2001), 3—Boiron et al. (1990), 4—Boiron et al. (2001), 5—Boiron et al. (1996).
* Indicates that bulk compositions have been calculated without NaCl.

some of the studied deposits (Boiron et al., 1992); and (iii) dilution of the c–w fluids by waters free of volatiles.

5.2. Aqueous fluids: salinity–Th evolution

Tm ice–Th plots (Fig. 4) summarise the evolution of aqueous fluids in the studied deposits. Aqueous fluids were trapped mostly as fluid inclusions in microfissures characterised by single Th–Tm pairs which, when the whole set of data is considered, document a dilution trend of the earliest aqueous fluids. The Th range (130–280 °C) cannot be interpreted only as a result of pressure changes because: (i) the salinity is not constant and indicates that a mixing process has occurred, in which two end-members are identified. The first one had a moderate salinity (up to 9 eq. wt.% NaCl), the second one was more dilute (close to 0.5 eq. wt.% NaCl). The two end-members and a line showing the trend of mixing are evident in each diagram (Fig. 4). It is interesting to note that most of the data plot along this line or below, and show a significant and progressive decrease in fluid salinity. (ii) The range of Th is too large to be simply the result of a pressure change at constant temperature (lithostatic to hydrostatic transition would yield a maximum fluctuation of around 60 °C) and indicates the mixing of two fluids with distinct temperatures. Mixing was probably mostly adiabatic, although the degree of thermal equilibrium with the host rocks is unknown. These processes are well illustrated in the Tm ice–Th plot from Tomino and Fagassière, among others, which show first a decrease in Th at subconstant Tm ice, followed by a significant decrease in Tm ice at slightly decreasing Th. In all studied examples, fluid circulation in faults ended with low salinity fluids, which corresponds to the latest microcracking stage in all the gold-bearing samples.

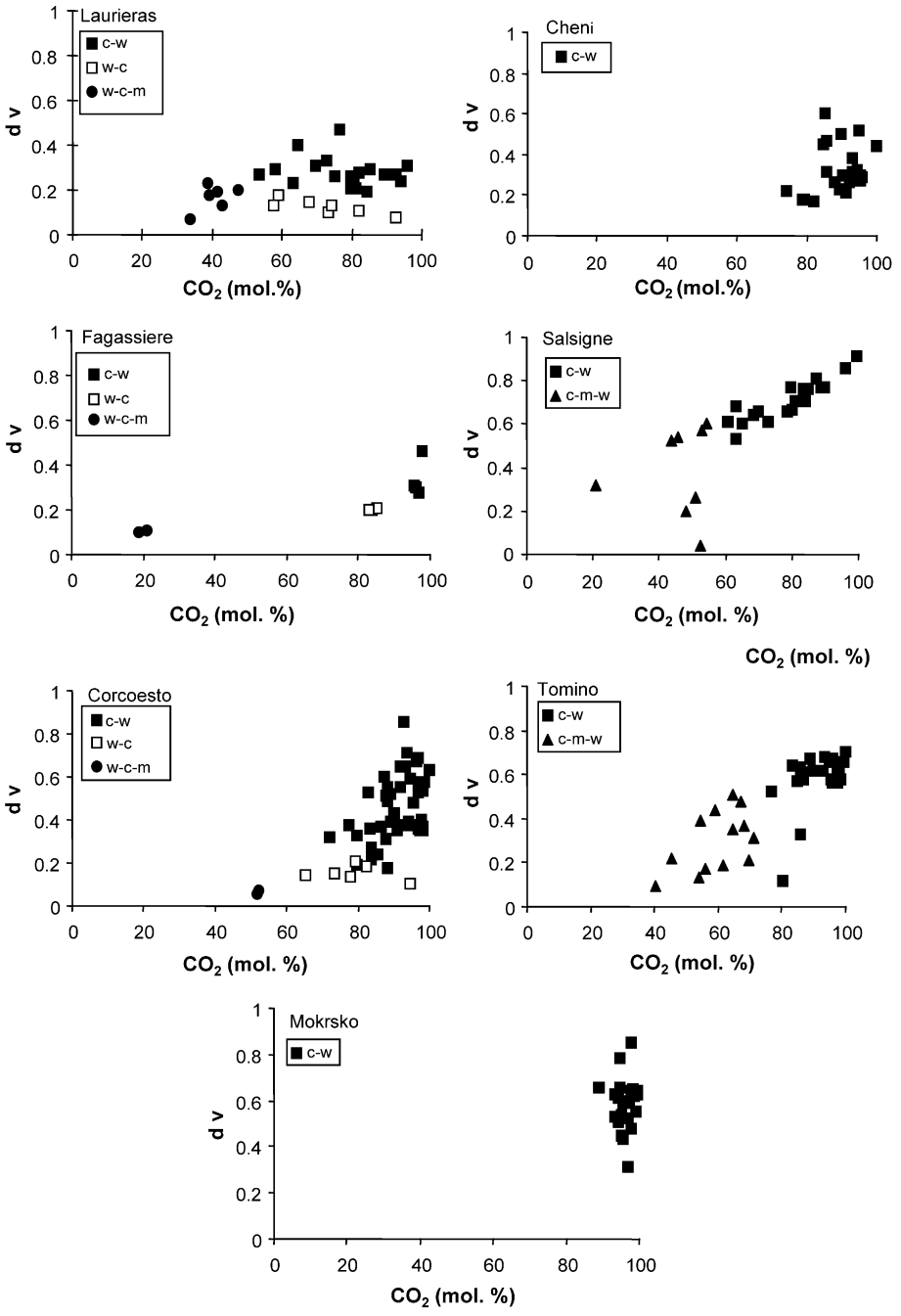

Fig. 2. Density of the volatile phase (dv) versus CO_2 (mol%) plots of aqueous carbonic fluids from each of the studied deposits.

In the case of the Salsigne deposit, the mixing process is not clearly observed. Most of the aqueous fluids have low salinity (up to 2 eq. wt.% NaCl) and Th covers a relatively wide range (120–300 °C) suggesting repeated reopening of the microcracks. However, some fluid inclusions with a higher salin-

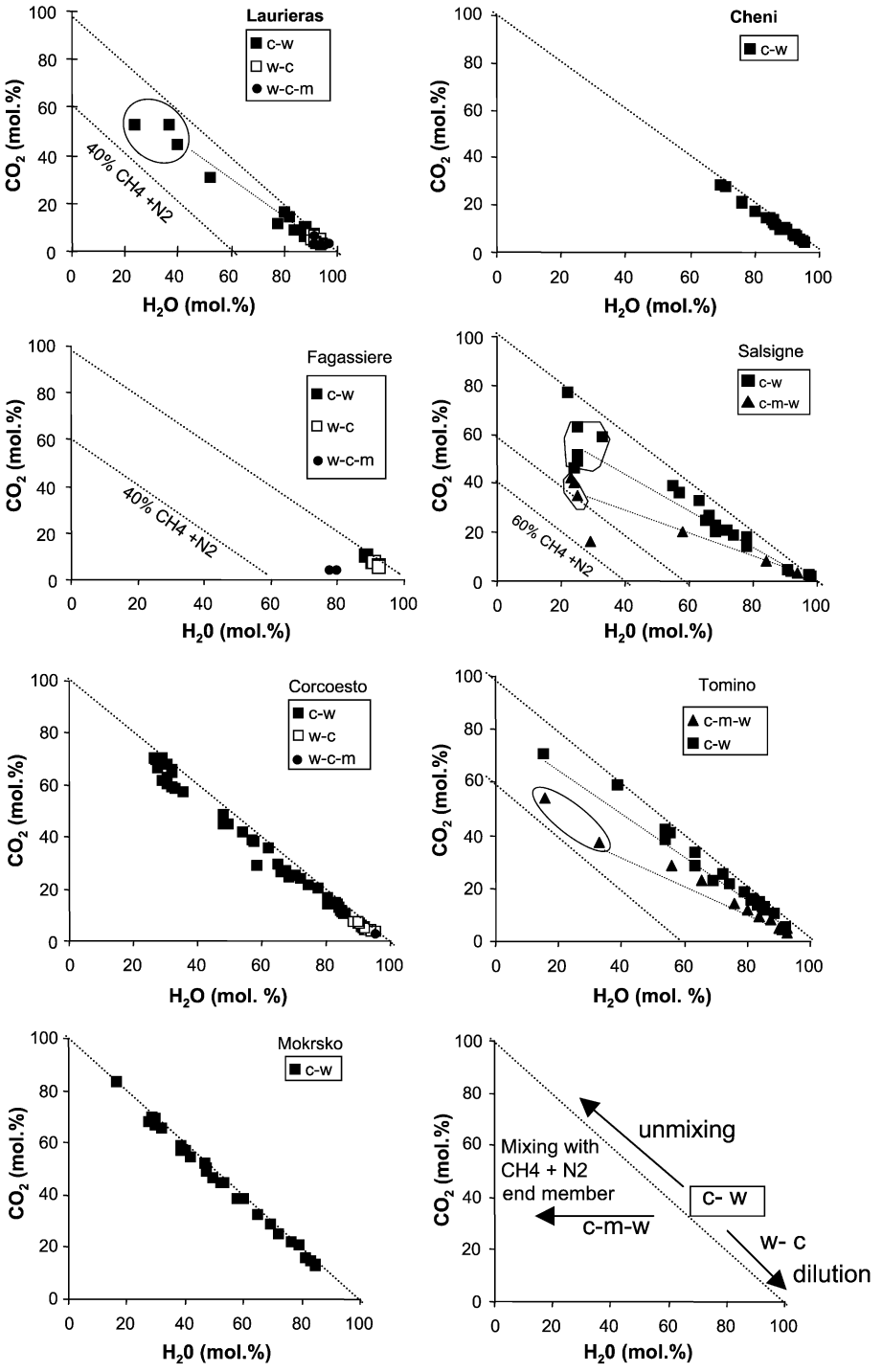

Fig. 3. H_2O (mol%) versus CO_2 (mol%) plots of the bulk composition of aqueous carbonic fluids from each of the studied deposits.

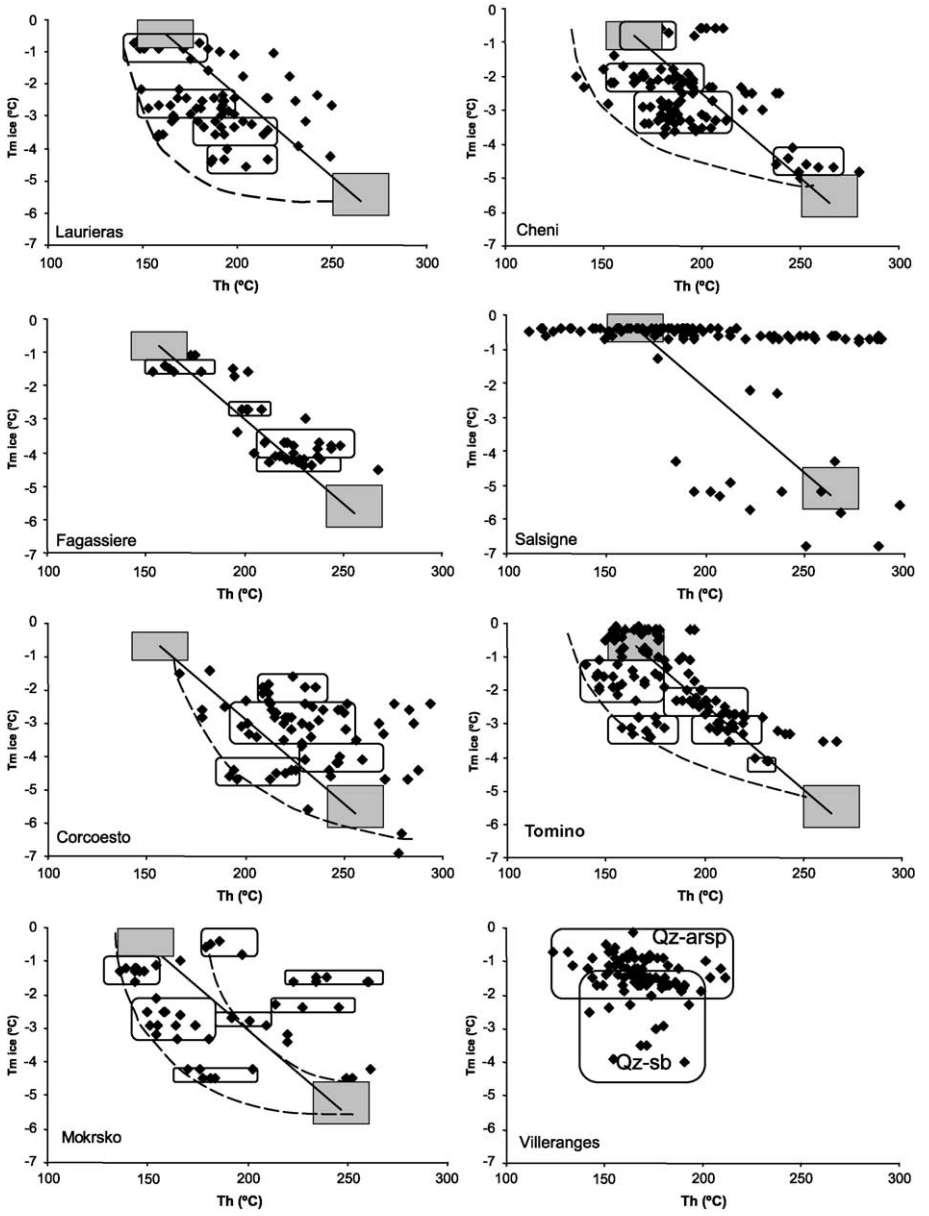

Fig. 4. Tm ice versus Th plots of aqueous fluid inclusions. The two boxes in gray show the possible end-members at Lauriéras, and were reproduced identically in all the diagrams as a guide for interpretation. For the Villeranges deposit, fluids associated with the two mineral assemblages are distinguished: quartz–arsenopyrite: Qz–arsp, quartz–stibnite: Qz–sb.

ity, in the range of 6–10 eq. wt.% NaCl, are found locally.

One exception is the case of the Villeranges and Chatelet deposits, where aqueous fluids are observed in authigenic quartz crystals. They have characteristics (salinity and Th) very similar to those recorded for late aqueous fluids from mesothermal deposits. The salinity is less than 4 eq. wt.% NaCl and Th

ranges from 140 to 240 °C (Boiron et al., 1989, 1990).

Low salinity (<1 eq. wt.% NaCl)–low temperature (Th ≈ 100–150 °C) fluids characterise the late barren quartz.

6. *P–T* evolution

The main *P–T* evolution pathways have already been discussed elsewhere (Boiron et al., 1996, 2001; Essarraj et al., 2001) and are only summarised below. The early activity of the faults and the earliest quartz deposition occurred at high temperatures (generally >400 °C) within a pressure range of 200–450 MPa. The highest pressures (350–450 MPa) were determined for inclusions found in quartz from the wall rocks of the mineralised faults (Lauriéras, for example) which indicates that this part of the basement was still located at a rather deep structural level (13–17 km) at the end of the Variscan collision stage (Essarraj et al., 2001). In NW Iberia and in Bohemia, pressures for the vein formation were lower but could reach 380 MPa giving a maximum estimated depth of around 15 km (Fig. 5).

One of the specific features of late Hercynian deposits is the relatively long-lived drainage of the same volume of rock, which was either centered on a fault zone, and its immediate boundaries (Lauriéras, Cheni, Fagassière, Salsigne (Fontaine de Santé fault)), or related to a network of subparallel joints (Mokrsko, Corcoesto, Tomino) formed within the granite at some distance from major faults or shear zones. The fault acted as a trap for several stages of mineralisation. The aqueous carbonic fluids associated with the As–S stage were trapped under lower *P–T* conditions which were respectively 50–180 MPa and 350–450 °C. The pressure decrease from the earlier stage documents an uplift of 5 to 10 km (Boiron et al., 1996, 2001; Vallance, 2001). At this time, apparent geothermal gradients were necessarily high owing to the rather high temperatures (400±50 °C) still recorded in the rock pile for a fluid pressure indicative of rather shallow structural levels. The latest stage is characterised by the mixing of a moderately saline end-member, probably issued from the evolution of fluids

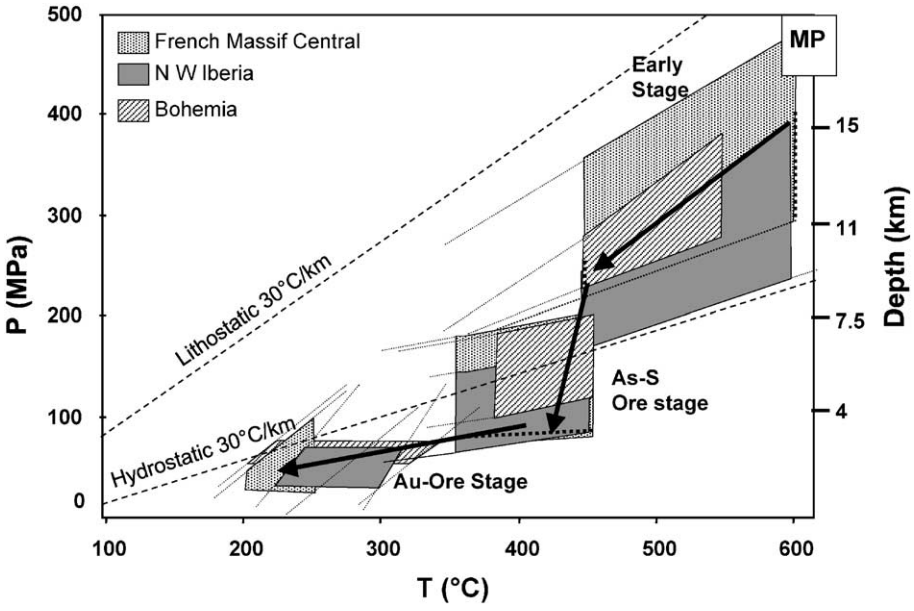

Fig. 5. General *P–T* reconstruction of the conditions prevailing in the three studied zones of the Variscan orogen. Depth has been calculated assuming a lithostatic pressure (density of the rock pile of 2.6 g/cm^3).

from the deep reservoir, by dilute fluids of lower temperature. Mixing was probably favoured by the connection of fluid reservoir by faults, and is likely to have occurred under hydrostatic pressures, or at a pressure lower than those reached during the preceding stages.

7. Fluid sources

7.1. Halogen chemistry

The halogen data set (Table 5) consists of analyses carried out on quartz from NW Iberia (partially reported in Boiron et al., 1996), from Mokrsko (Boiron et al., 2001) and from the French Massif Central (new data on Lauriéras, Salsigne, Villeranges and Chatelet).

The halogens, Cl, Br and, to a lesser extent I, can be used to distinguish fluids from different sources (Böhlke and Irwin, 1992) because these are conservative anionic species which are relatively unaffected by fluid–rock interactions (e.g., Banks et al., 1991). The reason for that behaviour is the fact that in a low salinity fluid, such as seawater, the concentrations of Cl and Br (19 000 and 65 ppm, respectively) are much higher than in crustal rocks (crustal averages of 130 and 2.5 ppm, respectively). So, the Br/Cl ratio remains constant in the event of fluid–rock interaction while this process induces a change of the I/Cl ratio because the concentration of I is lower in seawater than in crustal rocks (0.06 and 0.5 ppm, respectively).

The fluid chemistry was investigated on bulk samples and corresponds to mixed fluid populations for most of them. Thus, it is difficult to evaluate the contribution of the aqueous fluid-type to the bulk analysis, since the earlier fluid types also contain liquid water, and are contributing, in part, to the bulk anion and cation fluid chemistry. From their halogen composition, most of the fluids found in quartz veins appear to have equilibrated with upper crustal rocks, such as fluids from the deep Canadian or Baltic shields (Frape and Fritz, 1987). log Br/Cl values in the inclusion fluids are significantly higher than seawater and are in the range from −2.2 to −3 for most of the samples. The aqueous-carbonic fluids have halogen signatures similar to those of many upper crustal fluids including shield brines (Frape and Fritz,

Table 5
log Br/Cl and log I/Cl (mole ratios) obtained from crush leach analyses of fluid inclusions, with indication of the dominant fluid type in the analysed quartz

Location	Samples	Dominated fluid	Br/Cl (10^4)	I/Cl (10^4)
French Massif Central				
Lauriéras	Lau-2	w	4.78	0.31
	Lau-8	w	7.85	0.58
	Lau-9	w	10.2	1.48
	Lau-10b	w	10.9	0.72
	Lau-11	w	3.23	0.31
Salsigne	Sal-7	c–w	38.9	0.17
	Sal-10	c–w	67.6	0.02
	Sal-12	c–w	46.7	0.02
	Nesp-1	c–w	64.5	0.02
	Cum	c–w	12.3	0.24
Villeranges	Vil-1	w	2.69	0.44
	Vil-2	w	1.14	0.32
	Vil-50	w	30.2	0.48
	3183	w	35.4	0.41
	56	w	28.8	0.47
Chatelet	34	w	3.1	0.62
	Ch3	w	2.69	0.26
Bohemian Massif				
Mokrsko (1)	Mok 5	c–w+w	12.82	0.53
	Mok 6	c–w+w	20.53	0.59
	Mok 30–33	c–w+w	15.87	0.55
North Western Iberia				
Corcoesto (2)	cor-10	c–w	16.60	0.11
	181–80	c–w	21.33	0.30
	323–30	c–w	17.03	0.04
	348–60	c–w	27.58	0.15
	419–70	c–w	28.79	0.10
	464–30	c–w	14.89	0.20
	527–00	(c–w)+w	11.12	0.20
	527–60	(c–w)+w	8.20	0.08
Tomino (2)	1	c–w	30.96	0.04
	2	c–w	45.66	0.22
	3	c–w	37.17	0.27
	4	c–w	40.82	0.62
	5	c–w	41.67	0.13
	7	c–w	30.96	0.52
	8	c–w	51.28	0.13
	9	c–w	52.63	0.11
	10	c–w	21.88	0.41
	12	c–w	45.66	0.65
	13	c–w	37.17	0.68
	14	c–w	37.17	0.30
	16	c–w	47.85	0.03

1—Data from Boiron et al. (2001); 2—data from Boiron et al. (1996).

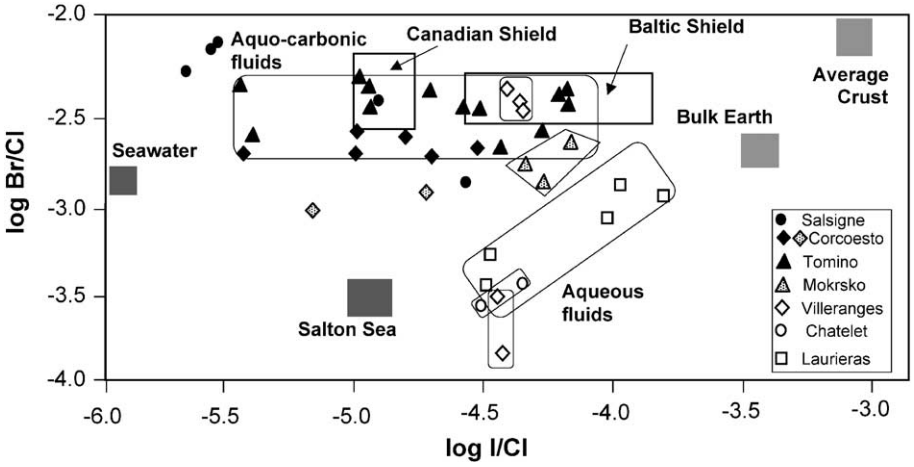

Fig. 6. log Br/Cl vs. log I/Cl (mole ratios) plot for crush leach analyses obtained on gold-bearing quartz veins. Also shown are results for other crustal fluids from literature (Frape and Fritz, 1987; Böhlke and Irwin, 1992). Dark symbols: aqueous-carbonic dominated fluids, white symbols: aqueous dominated fluids, dotted symbols: mixed fluids (aqueous-carbonic+aqueous fluids).

1987). Such Br/Cl ratios are quite similar to those reported for the Muruntau Au-bearing quartz veins where log Br/Cl values range from −2.4 to −3.4 (Graupner et al., 2001). They are also comparable to those measured for Brusson (Yardley et al., 1993) and Alleghany (Böhlke and Irwin, 1992) Au-bearing quartz veins. log I/Cl values lie in between −4 and −5.5 (Figs. 6 and 7; Table 5). However, a few samples show lower log Br/Cl values ranging from −3.5 to −4 attesting to rather low Br contents. Samples with Br-depleted values, relative to the Br/Cl ratio of seawater, are dominated by the aqueous fluid population. They are two samples from Corcoesto deposit, the ore-bearing quartz from Lauriéras, as well as the Au–arsenopyrite-bearing quartz from Chatelet and Villeranges.

The halogen composition suggests that the salt component of the early aqueous-carbonic fluids evolved in a low water–rock ratio setting, as found in modern shield brines. The last stage is characterised

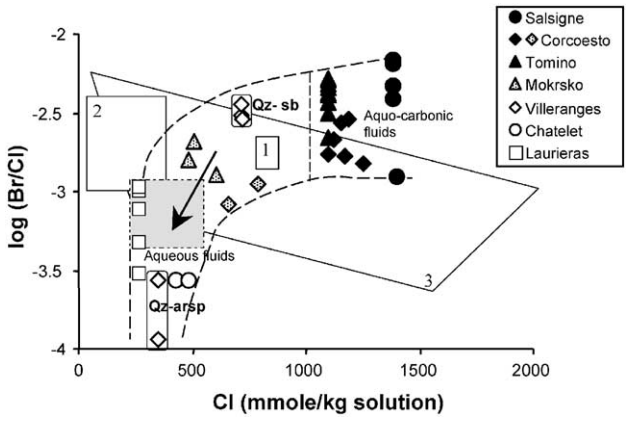

Fig. 7. log Br/Cl vs. Cl plot for crush leach analyses obtained on gold-bearing quartz veins. Results from gold deposits reported in the literature are also presented for comparison. Symbols are the same as in Fig. 6. (1) Brusson Au–quartz veins (Yardley et al., 1993), (2) Alleghany Au–quartz veins (Böhlke and Irwin, 1992), (3) Muruntau Au–quartz veins (Graupner et al., 2001). Qz–sb: quartz–stibnite mineralisation and Qz–arsp: quartz-arsenopyrite (Villeranges-Chatelet). The square in gray shows the range of Cl content for Lauriéras fluids.

by a progressive dilution of the crustal fluids by solutions penetrating the basement from the surface and having low Br/Cl ratios (Fig. 7).

7.2. Origin of fluids: O isotope geochemistry of quartz

The O isotopic data base was acquired on bulk quartz samples and also on separated quartz chips extracted from fluid inclusion wafers in order to single out the isotopic signature of each stage identified on the basis of FI studies. This approach was not possible for H in the purpose of identifying the isotopic signatures and possibly the primary origin of the fluid involved in the gold deposition stage. This is because Variscan gold deposit systems do not contain OH-bearing mineral species attributable to the gold deposition stage and on the fact that high precision D/H analysis of fluid inclusions requires large samples of monophase quartz devoid of any minute amounts of OH-bearing minerals, which were not available. Thus, attempts to interpret the evolution of the quartz O isotopic composition were carried out using the constraints deduced from the fluid chemistry.

The first type of fluids (H_2O-CO_2, $H_2O-CO_2-CH_4$ fluids) was trapped in milky quartz and microcrystalline quartz, and may be related to the main sealing stages affecting the faults. The O isotopic compositions (Table 6) are akin to those measured in many large mesothermal deposits worldwide (e.g., Kerrich, 1987 and references therein). Estimated $\delta^{18}O$ fluid values range from 8‰ to 12.5‰ (Table 6 and Fig. 8), considering crystallisation or reequilibration temperatures between 400 and 500 °C. Such values are characteristic of fluids isotopically in equilibrium with common basement materials at medium to high temperatures (≥400–500 °C). These values may correspond to magmatic (derived from granitoids), metamorphic (dehydration during prograde metamorphism) or "pseudo-metamorphic" fluids (i.e., any kind of H_2O-bearing fluid isotopically equilibrated with crustal reservoirs under low fluid/rock ratios). However, we suggest that a magmatic origin is unlikely because, in such a case, the original fluid should have lost the whole of its primary characteristics (salinity, geochemical markers such as the Li content, elemental ratios of conservative elements such as the halogens).

The $\delta^{18}O$ values calculated for the aqueous fluids are estimated in the range 0.3–6‰, based on temperatures between 150 and 250 °C, assuming that the related quartz types are in equilibrium with these fluids, which is reasonable when these quartz are found to be newly formed at that stage. This is generally the case but in one instance (Lauriéras; Essarraj et al., 2001), the situation may be more complex. In the case of "epithermal" deposit (Villeranges), the isotopic signature could be even lighter ($\delta^{18}O$=−1‰ to +4‰). Such values are indicative of a meteoric origin for the fluid, considering that during

Table 6
Summary of the O stable isotope data ($\delta^{18}O$‰ vs. SMOW) for the Au–quartz veins in the French Massif Central

Location	Type of quartz	$\delta^{18}O$ quartz (‰)	Estimated T (°C)	$\delta^{18}O$ fluid (‰)
Lauriéras (1)	mkQ±cQ	13.3/14.8	450–500	9.6/11.7
	mkQ±mQ	12.7/14.7	450–500	9.0/11.6
	mQ	13.5	450–500	9.8/10.5
	cQ	16.5	230	6.6
Cheni (2)	mkQ	15.2/16.2	400–450	10.7/12.5
	mcQ	12.2/12.9	415–425	7.9/8.8
	hQ	13.1	360–400	7.7/8.6
	cQ	11.9/13.4	200–240	0.3/4
Fagassière (2)	mkQ	15.4	400–450	10.9/11.7
	mcQ	15.4	400–450	10.9/11.7
	hQ	15.7	350–400	10.1/11.2
	lbQ	21.5	100–150	0.3/6
Villeranges	Q–arsp	10.6/13.6	200–240	−1.0/4

mkQ: Milky quartz, mQ: microcystalline quartz, cQ: clear quartz, hQ: hyaline quartz, lbQ: late barren quartz, Q: quartz, arsp: arsenopyrite. Data have been completed or synthetised from 1—Essarraj et al. (2001) and 2—Vallance (2001).

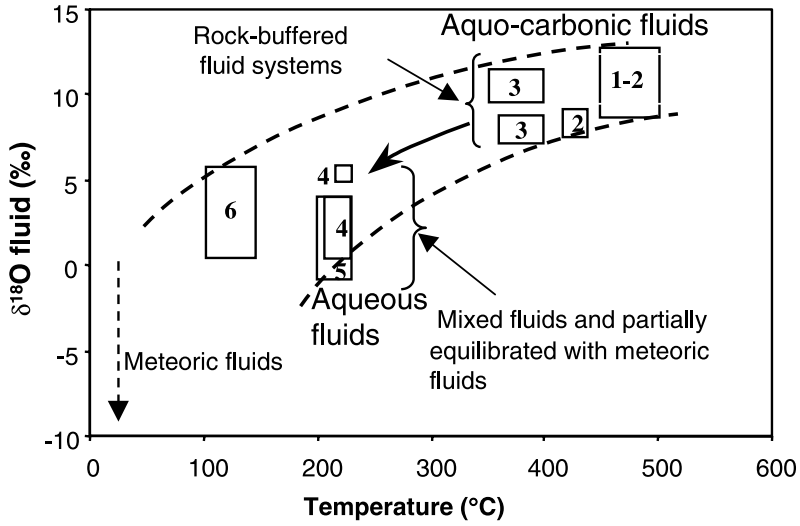

Fig. 8. Diagram showing the fields of $\delta^{18}O$ values (calculated from quartz isotopic data) and measured temperatures (fluid inclusions studies) for the successive stages of quartz growth and reequilibration identified in the gold-bearing quartz veins from the French Massif Central. (1) Milky quartz, (2) micro-crystalline quartz, (3) hyaline quartz, (4) clear quartz, (5) quartz–arsenopyrite, (6) late barren quartz (see Table 5).

infiltration and heating, groundwater may become somewhat ^{18}O-enriched through fluid/rock interaction. Nonetheless, equilibration of metamorphic (or pseudo-metamorphic) fluids with basement rocks down to very low temperatures under low fluid/rock ratios may also theoretically produce isotopic compositions in this range. For example, H_2O isotopically buffered by K-feldspar with $\delta^{18}O$=+9 ‰ (a common value for granitoid and basement rocks) would have a $\delta^{18}O$ of −2 ‰ to +4 ‰ in the temperature range 150–250 °C (using Zheng's, 1993 equations). The lower "limit" of the field of isotopic compositions ascribed to metamorphic fluids is debatable but is never extended to $\delta^{18}O$ values around 0, even by those authors who extend that field to extreme values (e.g., Kyser and Kerrich, 1990). So, a meteoric origin is the most probable option, but we really do not have firm constraints (particularly considering the kinetics of isotopic equilibration in natural conditions) on the "closure" temperature for such a metamorphic fluid system. Once again, therefore, additional constraints on the fluid chemistry are useful in helping to explain O isotopic data.

The gold deposition stage is rarely accompanied by major quartz growth, except in the "epithermal" Villeranges deposit where isotopically light fluids were involved. In the Lauriéras deposit (Essarraj et al., 2001), reequilibration of early quartz with fluids related to the gold stage suggests that the latter was accompanied by a drop in the fluid $\delta^{18}O$ value (down to ca. +6.5 ‰). As a whole, gold deposition seems to be associated with the onset of a transition between a flux of metamorphic fluids, with common O isotopic compositions, to a flux of fluids with lighter O isotopic signatures. This decrease is thus indicative of a switch in the *P*, *T*, *X* conditions and/or modalities of fluid flow that may help our understanding of the mechanism of gold deposition. Three types of processes can be envisaged: (i) mixing of resident "pseudo-metamorphic" fluids equilibrated with basement rocks at very different temperatures (typically, 350–450 °C on the one hand and 150–250 °C on the other), and (ii) unmixing and loss of a large fraction of CO_2 from the aqueous carbonic fluids (e.g., Higgins and Kerrich, 1982). Actually, this latter process alone is not expected to produce the isotopic effects commensurate with those recorded (up to ca. 10 ‰ overall depletion at some sites). Moreover, fluid unmixing is not documented as a major process in the whole of the Variscan gold deposits studied so far (see above). (iii) Dilution by a low $\delta^{18}O$ hydrothermal fluid of surface derivation.

To conclude based on the isotopic arguments, we estimate that scenario (i) above is flawed by uncer-

tainties related to the production of the low ^{18}O fluid end-member, by the physical difficulty of associating, in the same place, fluids which experienced retrograde equilibration down to very different temperatures (and thus depths) and finally, inconsistency with the chemical evolution of the fluids studied. The existence of fluids of both deep and surficial derivation and dilution of the hot pseudo-metamorphic fluid by surficial fluids seems to be the most likely process linked to gold deposition in the different gold districts studied. Mixing between descending and ascending fluids in the late stage of quartz lode evolution is also consistent with the brittle regime that prevailed in the basement during decompression and provided easy pathways for the fluids.

8. Discussion and conclusion

Au-bearing quartz in late Hercynian lode deposits display some constant features all over Europe (Galicia in Spain, Portugal, French Massif Central, Bohemian Massif) in terms of (i) timing of gold introduction or enrichment and its specific association with small amounts of Bi, Pb, Cu minerals, (ii) nature of the fluids and their geochemical features, and (iii) degree of equilibration with the basement of the two main fluid types involved.

8.1. Fluid origin

All the available data suggest that the early fluids related to the origin of the primary faults sealing were extensively equilibrated with the metamorphic series whatever their ultimate origin (pseudo-metamorphic fluids). The fluids involved during early development are characterised by a high Br/Cl ratio, $CH_4/CO_2/H_2O$ ratios rather typical of fluids equilibrated with graphite, and moderate to medium salinities. From these characteristics, it appears that the late Hercynian Au deposits share a part of their history with typical Au mesothermal deposits worldwide (Groves et al., 1998; Dugdale and Hagemann, 2001). The main driving process for fracture sealing was thus ascending flow of waters, equilibrated with the metamorphic pile, along the faults, as shown in Fig. 9a. The likely mechanism to precipitate silica was a drop in fluid pressure, as quartz solubility is highly dependant on pressure in the 400–500 °C range (Walther and Helgeson, 1977; Cox et al., 1991). It is possible that these early fluids experienced a moderate increase in chlorinity linked to the hydration of minerals such as biotite, alteration of feldspars into phengite during the fluid–rock interaction around faults. In any case, we must consider the possibility that scavenging of gold from large crustal volumes was carried out by this type of fluid which then flowed into localised, and very small, crustal domains as suggested for the Yilgarn Craton by Cox (1999). The main stage of gold deposition is not however linked to the main sealing stages of the fault.

Although granites are present in the surroundings of most studied deposits, they cannot be considered as granite-related gold deposits in the sense of Lang and Baker (2001).The granitoids act as sources of heat that drive thermal convection cells in which fluids scavenge gold and other metals as suggested by Rowins et al. (1997) for gold mineralisations in the Telfer dome (Western Australia).

8.2. Evolution and timing of fluid compositions in the active faults

The main feature of the sealing process and of Au deposition is the long-lived activity of the fault and of fluid percolation, until the fault connected the two distinct fluid reservoirs at a critical stage of the basement uplift. In the model favoured here, the shallow-seated reservoir corresponded to a fluid cell in which surface-derived waters percolated into the basement along short pathways, which precluded total equilibration with the microfractured host rocks. At that stage, fluids evolved by two main mechanisms: (i) drop of temperature accompanying decompression which induced in some instances volatile unmixing at the end of the decompression event in the faulted systems and (ii) mixing of the resulting fluids with waters entering, or present in, the shallower reservoir (Fig. 9b). The constancy of the data is indicative of a long but similar fluid history at the province scale (Boiron et al., 1996, 2001; Essarraj et al., 2001).

As a whole, the $P–T–X$ fluid evolution reflects a series of major changes which are, in turn, connected with the global evolution of the Variscan belt. The

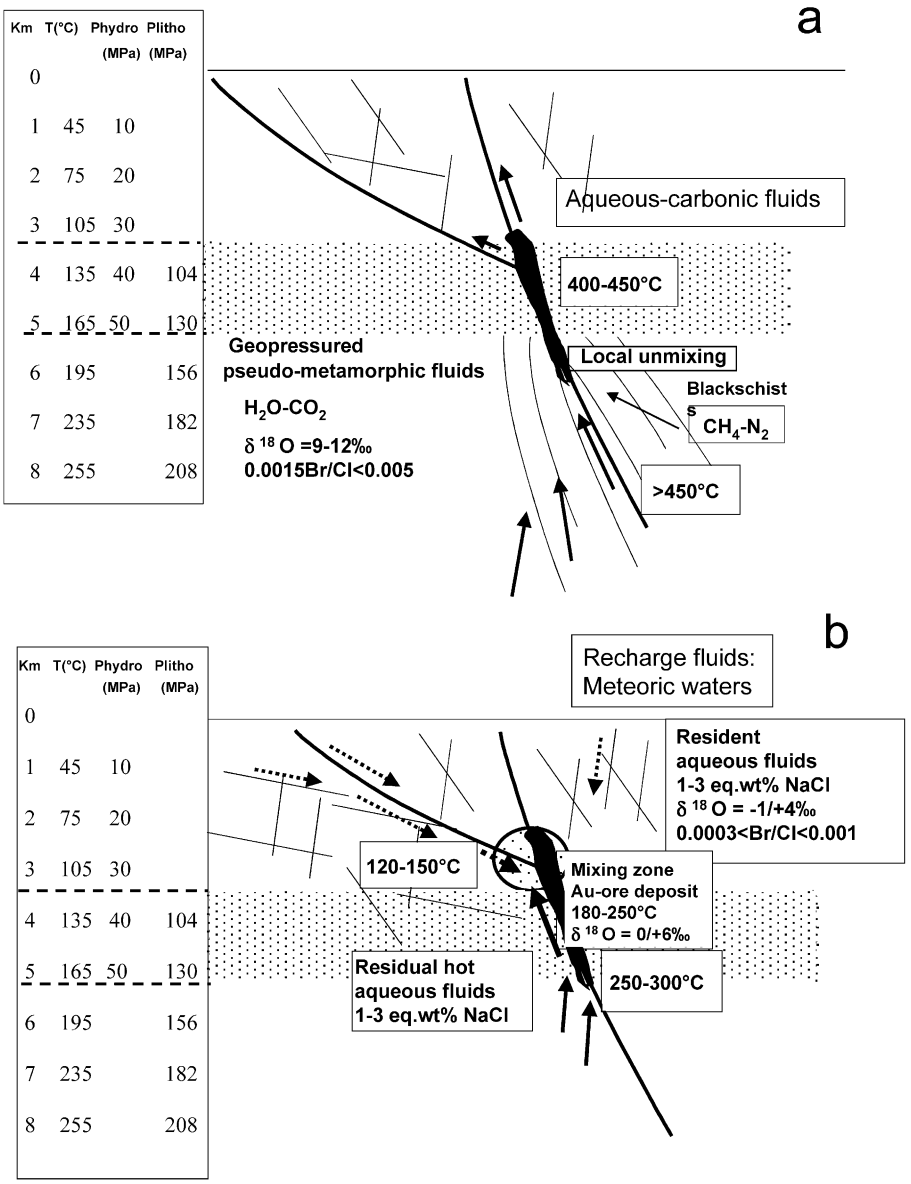

Fig. 9. Two-stage model of the fluid circulation in and around the faults active during the uplift. Reference temperatures and pressures (in columns) at a given depth were calculated using a thermal gradient of 30 °C/km and an average density of the rock pile of 2.6 g/cm^3.

Hercynian uplift crisis has produced a sudden link between two major fluid reservoirs, with oscillatory or rapid changes in pressure (lithostatic to hydrostatic) and temperature due to advection of cool fluids from shallower levels. In this context, dilution and mixing appear to be the most probable factor decreasing gold solubility together with a pressure drop (Gibert et al., 1998), allowing Au deposition and trapping by early deposited sulphides. Thus, the major geodynamic switch towards generalised extensional tectonics that occurred during the uplift and thinning of the upper crust after the collisional stages may be the key factor controlling Au deposition in the late Hercynian gold deposits.

Acknowledgements

The authors thank A. Rankin, A.M. Boullier and F. Noronha for helpful comments of the manuscript. This work has been partially supported by CDR TRANSMET. **[RR]**

References

Arias, D., Martin-Izard, A., 2000. An introduction to the typological characteristics of gold deposits in NW Iberian Peninsula. A geode-geofrance 3D workshop on orogenic gold deposits in Europe with emphasis on the Variscides, Doc. BRGM. 297, pp. 89–93.

Bakker, R.J., 1997. Clathrates: computer programs to calculate fluid inclusion $V–X$ properties using clathrate melting temperatures. Comput. Geosci. 23, 1–18.

Banks, D.A., Davies, G.R., Yardley, B.W.D., McCaig, A.M., Grant, N.T., 1991. The chemistry of brines from an Alpine thrust system in the Central Pyrenees: an application of fluid inclusion analysis to the study of fluid behaviour in orogenesis. Geochim. Cosmochim. Acta 55, 1021–1030.

Benchekroun, F., Berger, G., Moine, B., 1996. Un modèle minéralogique et chimique du dépôt de l'or dans le gisement de Salsigne (Montagne Noire). C. R. Acad. Sci. 323, 129–136.

Bodnar, R.J., 1993. Revised equation and table for determining the freezing point depression of H_2O–NaCl solutions. Geochim. Cosmochim. Acta 57, 683–684.

Böhlke, J.K., Irwin, J.J., 1992. Laser microprobe analysis of Cl, Br, I, and K in fluid inclusions: implications for sources of salinity in some ancient hydrothermal fluids. Geochim. Cosmochim. Acta 56, 203–226.

Boiron, M.C., Cathelineau, M., Trescases, J.J., 1989. Conditions of gold-bearing arsenopyrite crystallization in the Villeranges basin, Marche-Combrailles shear zone, France. A mineralogical and fluid inclusion study. Econ. Geol. 84, 1340–1362.

Boiron, M.C., Cathelineau, M., Dubessy, J., Bastoul, A.M., 1990. Fluids in Hercynian Au-veins from the French Variscan belt. Min. Mag. 54, 231–243.

Boiron, M.C., Essarraj, S., Sellier, E., Cathelineau, M., Lespinasse, M., Poty, B., 1992. Identification of fluid inclusions in relation to their host microstructural domains in quartz by cathodoluminescence. Geochim. Cosmochim. Acta 56, 175–185.

Boiron, M.C., Cathelineau, M., Banks, D., Yardley, B., Noronha, F., Miller, F.M., 1996. $P–T–X$ conditions of fluid penetration in the basement during retrograde metamorphism and uplift: a multidisciplinary investigation of bulk and individual fluid inclusion chemistry from NW Iberian quartz veins. Geochim. Cosmochim. Acta 60, 43–57.

Boiron, M.C., Barakat, A., Cathelineau, M., Banks, D.A., Durisova, J., Moravek, P., 2001. Geometry and $P–V–T–X$ conditions of microfissural ore fluid migration: the Mokrsko gold deposit (Bohemia). Chem. Geol. 173, 207–225.

Bottrell, S.H., Yardley, B.W.D., Buckley, F., 1988. A modified crush–leach method for analysis of fluid inclusion electrolytes. Bull. Mineral. 111, 279–290.

Bouchot, V., Gros, Y., Bonnemaison, M., 1989. Structural controls on the auriferous shear zones of the Saint Yrieix district, Massif Central, France: evidence from the Le Bourneix and Laurieras gold deposits. Econ. Geol. 84, 1315–1327.

Bouchot, V., Milesi, J.P., Ledru, P., Lerouge, C., Roig, J.Y., Bellot, J.P., Becq-Giraudon, J.F., Truffert, C., 2000. Orogenic gold veins and W, Li–F mineralizations related to "specialised" granites: two markers of the crustal scale Au–W–Sb metalliferous peak at 310–305 Ma (French Variscan Belt). A geode-geofrance 3D workshop on orogenic gold deposits in Europe with emphasis on the Variscides, Doc. BRGM 297, pp. 53–55.

Cathelineau, M., Boiron, M.C., Holliger, P., Marion, P., Denis, M., 1989. Gold in arsenopyrites: crystal chemistry, location and state, physical chemical conditions of deposition. Econ. Geol., Monograph 6, "The geology of gold deposits: the perspective in 1988", pp. 328–340.

Cathelineau, M., Boiron, M.C., Essarraj, S., Dubessy, J., Lespinasse, M., Poty, B., 1993. Fluid pressure variations in relation to multistage deformation and uplift: a fluid inclusion study of Au–quartz veins. Eur. J. Mineral. 5, 107–121.

Clayton, R.N., Mayeda, T.K., 1963. The use of bromine pentafluorine in the extraction of oxygen from oxides and silicates for isotopic analysis. Geochim. Cosmochim. Acta 27, 43–52.

Cox, S.F., 1999. Deformational controls on the dynamics of fluid flow in mesothermal gold systems. In: Mc Caffrey, K.J.W., Lonergan, L., Wilkinson, J.J. (Eds.), Fractures, Fluid Flow and Mineralisation. Geological Society, vol. 155, pp. 123–140. Special Publications, London.

Cox, S.F., Wall, V.J., Etheridge, M.A., Potter, T.F., 1991. Deformational and metamorphic processes in the formation of mesothermal gold deposits. Examples from Lachlan Fold Belt in central Victoria, Australia. Ore Geol. Rev. 6, 391–423.

Dubessy, J., 1984. Simulation des équilibres chimiques dans le système C–O–H. Conséquences méthodologiques pour les inclusions fluides. Bull. Mineral. 107, 157–168.

Dubessy, J., Poty, B., Ramboz, C., 1989. Advances in the C–O–H–N–S fluid geochemistry based on micro-Raman spectroscopic analysis of fluid inclusions. Eur. J. Mineral. 1, 517–534.

Dugdale, A.L., Hagemann, S.G., 2001. The Bronzewing lode-gold deposit, Western Australia: $P–T–X$ evidence for fluid immiscibility caused by cyclic decompression in gold-bearing quartz veins. Chem. Geol. 173, 59–90.

Duthou, J.L., Cantagrel, J.M., Didier, J., Vialette, Y., 1984. Paleozoic granitoids from French Massif Central: age and origin studied by $^{87}Rb/^{87}Sr$ system. Phys. Earth Planet. Inter. 35, 131–144.

Essarraj, S., Boiron, M.C., Cathelineau, M., Fourcade, S., 2001. Multistage deformation of Au–quartz vein: evidence for late gold introduction from microstructural, isotopic and fluid inclusion studies. Tectonophysics 336, 79–99.

Floc'h, J.P., 1983. Le socle métamorphique du Limousin central: une traverse de la zone ligérienne de l'orogenèse varisque de l'Aquitaine à la zone broyée d'Argentat (Massif Central franç ais). Unpub. thesis, Limoges Univ.

Frape, S.K., Fritz, P., 1987. Geochemical trends for groundwaters from the Canadian shield. In: Fritz, P., Frape, S.K. (Eds.), Saline Water and Gases in Crystalline Rocks. Geol. Assoc. Canada Spec. Pap., vol. 33, pp. 19–38.

Gibert, F., Pascal, M.L., Pichavant, M., 1998. Gold solubility and speciation in hydrothermal solutions: experimental study of the stability of hydrosulfide complex of gold (AuHS°) at 350 °C and 500 bars. Geochim. Cosmochim. Acta 62, 2931–2947.

Graupner, T., Kempe, U., Spooner, E.T.C., Bray, C.J., Kremenetsky, A., Irmer, G., 2001. Microthermometric, laser Raman spectroscopic and volatile-ion chromatographic analysis of hydrothermal fluids in the Paleozoic Muruntau Au-bearing quartz vein ore field, Uzbekistan. Econ. Geol. 96, 1–23.

Groves, D.I., 1993. The crustal continuum model for late Archaean lode-gold deposits of the Yilgarn block, western Australia. Miner. Depos. 28, 366–374.

Groves, D.I., Goldfarb, R.J., Gebre-Mariam, M., Hagemann, S.G., Robert, F., 1998. Orogenic gold deposits, a proposed classification in the context of their crustal distribution and relationship to other gold deposit types. Ore Geol. Rev. 13, 7–27.

Higgins, N., Kerrich, R., 1982. Progressive ^{18}O depletion during CO_2 separation from a carbon dioxide-rich hydrothermal fluid: evidence for the Grey River tungsten deposit. Can. J. Earth Sci. 19, 2247–2257.

Hubert, P., 1986. Textures et inclusions fluides des quartz aurifères. Application au gîte de Cros Gallet (Haute Vienne, France) et au prospect de Sanoukou (district de Kinieba, Mali). Doc. BRGM 114. 350 pp.

Iglesias, M., Chouckroune, P., 1980. Shear zones in the Iberian arc. J. Struct. Geol. 2, 63–68.

Jacobs, G.K., Kerrick, D.M., 1981. Methane: an equation of state with application to the ternary system $H_2O–CO_2–CH_4$ system. Geochim. Cosmochim. Acta 45, 607–614.

Kerrich, R., 1987. The stable isotope geochemistry of Au–Ag vein deposits in metamorphic rocks. In: Kyser, T.K. (Ed.), Stable Isotopes Geochemistry of Low Temperature Fluids. Min. Assoc. Canada, vol. 13, pp. 287–336.

Kerrick, D.M., Jacobs, G.K., 1981. A remodified Redlich–Kwong equation for $H_2O–CO_2$ and $H_2O–CO_2$ mixtures at elevated pressures and temperatures. Am. J. Sci. 281, 735–767.

Knipe, S.W., Foster, R.P., Stanley, C.J., 1991. Hydrothermal precipitation of precious metals on sulfide substrates. Proc. of Gold, vol. 91, pp. 431–435. A.A. Balkema, Brazil.

Kyser, T.K., Kerrich, R., 1990. Geochemistry of fluids in tectonically active crustal regions. In: Nesbitt, B.E. (Ed.), Fluids in Tectonically Active Regimes of the Continental Crust. Min. Assoc. Canada, vol. 18, pp. 133–230.

Lang, J.R., Baker, T., 2001. Intrusion-related gold systems: the present level of understanding. Miner. Depos. 36, 477–489.

Lépine, J., 1989. Le gisement sulfo-arsenié aurifère du cambrien inférieur de la mine traditionnelle de Salsigne (Montagne Noire, France). Contexte structural, métallogénique et sédimentologique. Unpub. thesis, Toulouse Univ., 243 pp.

Lescuyer, J.L., Bouchot, V., Cassard, D., Feybesse, J.L., Marcoux, E., Moine, B., Piantone, P., Tegley, M., Tollon, F., 1993. Le gisement aurifère de Salsigne (Aude, France): une concentration syntectonique tardivarisque dans les sédiments détritiques et carbonatés de la Montagne Noire. Chron. Rech. Min. 512, 3–73.

Marignac, C., Cuney, M., 1999. Ore deposit of the French Massif Central: insight into the metallogenesis of the Variscan collision belt. Miner. Depos. 34, 472–504.

Matte, P., 1991. Accretionary history and crustal evolution of the Variscan belt in western Europe. Tectonophysics 177, 151–170.

Möller, P., Kersten, G., 1994. Electrochemical accumulation of visible gold on pyrite and arsenopyrite surfaces. Miner. Depos. 29, 404–413.

Moravek, P., Janatka, J., Pertoldova, J., Straka, E., Durisova, J., Pudilova, M., 1989. The Mokrsko gold deposit—the largest gold deposit in the Bohemian Massif, Czechoslovakia. Econ. Geol. Monogr. 6, 252–259.

Noronha, F., Cathelineau, M., Boiron, M.C., Banks, D., Doria, A., Ribeiro, M.A., Nogueira, P., Guedes, A., 2000. A three-fluid stage model for Au metallogenesis in granites and their metamorphic host rocks in Northern Portugal. J. Explor. Geochem. 71, 209–224.

Piantone, P., Wu, X., Touray, J.C., 1994. Zoned hydrothermal alteration of the gold deposit at Le Chatelet (French Massif Central). Econ. Geol. 89, 757–777.

Poty, B., Leroy, J., Jachimowicz, L., 1976. Un nouvel appareil pour la mesure des températures sous le microscope: l'installation de microthermométrie Chaixmeca. Bull. Soc. Fr. Mineral. Cristallogr. 99, 182–186.

Robert, F., Brown, A.C., 1986. Archaean gold bearing quartz veins, at the Sigma Mine, Abitibi greenstone Belt, Quebec: Part II. Vein paragenesis and hydrothermal alteration. Econ. Geol. 81, 593–616.

Roedder, E., 1972. Composition of fluid inclusions. U.S. Geol. Surv., Prof. Paper 440JJ, 164 pp.

Rowins, S.M., Groves, D.I., McNaughton, N.J., Palmer, M.R., Eldridge, C.S., 1997. A reinterpretation of the role of granitoid in the genesis of Neoproterozoic gold mineralization in the Telfer dome, Western Australia. Econ. Geol. 92, 133–160.

Thiery, R., Vidal, J., Dubessy, J., 1994. Phase equilibria modelling applied to fluid inclusions liquid vapour equilibria and calculation of the molar volume in the $CO_2–CH_4–N_2$ system. Geochim. Cosmochim. Acta 58, 1073–1082.

Tollon, F., 1969. Le district aurifère de Salsigne (Aude). Unpub. thesis, Toulouse Univ., 176 pp.

Touray, J.C., Marcoux, E., Hubert, P., Proust, D., 1989. Hydrothermal processes and ore-forming fluids in the Le Bourneix gold deposit, Central France. Econ. Geol. 84, 1328–1339.

Vallance, J., 2001. Les paléofluides de la fin de la collision varisque: evolution pression–température–composition et rôle métallogénique. Une étude pluridisciplinaire des districts à Au d'Europe occidentale. Unpubl. thesis, Nancy I Univ., 326 pp.

Walther, J.V., Helgeson, H.C., 1977. Calculation of the thermodynamic properties of aqueous silica and the solubility of quartz and its polymorph at high temperatures and pressures. Am. J. Sci. 277, 1315–1351.

Yardley, B.W.D., Banks, D.A., Bottrell, S.H., Diamond, L.W., 1993. Post-metamorphic gold–quartz veins from N.W. Italy:

the composition and origin of the ore fluid. Min. Mag. 57, 407–422.

Zappettini, E.O., 1983. Le gisement d'or du Chatelet (Creuse, Massif Central Français). Cadre géologique régional, étude métallogénique. Unpub. thesis, Limoges Univ., 151 pp.

Zhang, Y.G., Frantz, J.D., 1987. Determination of the homogenization temperatures and densities of supercritical fluids in the system NaCl–KCl–$CaCl_2$–H_2O using synthetic fluid inclusions. Chem. Geol. 64, 335–350.

Zheng, Y.F., 1993. Calculation of oxygen isotope fractionation in anhydrous silicate minerals. Geochim. Cosmochim. Acta 56, 1079–1091.